

Generalizing plant–water relations to landscapes

R. H. Waring^{1,*} and J. J. Landsberg²

¹ College of Forestry, Oregon State University, Corvallis, OR 97331, USA

² Withycombe, Church Lane, Mt Wilson, NSW 2786, Australia

*Correspondence address. College of Forestry, Oregon State University, Corvallis, OR 97331, USA.

Tel: 541-737-6087; Fax: 541-737-1393; E-mail: richard.waring@oregonstate.edu

Abstract

Aims

Changing climate and land use patterns make it increasingly important that the hydrology of catchments and ecosystems can be reliably characterized. The aim of this paper is to identify the biophysical factors that determine the rates of water vapor loss from different types of vegetation, and to seek, from an array of currently available satellite-borne sensors, those that might be used to initialize and drive landscape-level hydrologic models.

Important Findings

Spatial variation in the mean heights, crown widths, and leaf area indices (LAI) of plant communities are important structural variables that affect the hydrology of landscapes. Canopy stomatal conductance (G) imposes physiological limitation on transpiration by vegetation. The maximum value of G (G_{\max}) is closely linked to canopy photosynthetic capacity, which can be estimated via remote sensing of foliar chlorophyll or nitrogen contents. G can be modeled as a non-

linear multiplicative function of: (i) leaf–air vapor pressure deficit, (ii) water potential gradient between soil and leaves, (iii) photosynthetically active radiation absorbed by the canopy, (iv) plant nutrition, (v) temperature and (vi) the CO_2 concentration of the air. Periodic surveys with Light Detection and Ranging (LiDAR) and interferometric RADAR, along with high-resolution spectral coverage in the visible, near-infrared, and thermal infrared bands, provide, along with meteorological data gathered from weather satellites, the kind of information required to model seasonal and interannual variation in transpiration and evaporation from landscapes with diverse and dynamic vegetation.

Keywords: canopy stomatal conductance • plant water relations • process-based models • remote sensing

Received: 21 September 2010 Revised: 17 December 2010

Accepted: 21 December 2010

INTRODUCTION

Increasing amounts of CO_2 are entering the atmosphere from burning fossil fuels and from conversions in land use round the world. This is causing changes in the way plant communities use water, so that the models we apply to calculate the hydrology of ecosystems, catchments, or forest stands are often found to be giving the wrong answers. To calculate transpiration, we need models based on variables that can be estimated from indirect measurements and applied at large scales. Satellites can provide information about changes in the surface properties of large areas, but they do not measure transpiration or evaporation directly. The properties for which we need values to do this include plant canopy characteristics, most importantly LAI and canopy conductance (G). Measures of solar radiation, temperature, and atmospheric vapor pressure deficit are also required. The short review presented here indicates that advances in remote sensing may allow us to measure the properties of vegetation that set limits on G , as well as seasonal

changes in the meteorological variables that affect transpiration and evaporation.

Changing patterns in vegetation and land cover can be mapped by instruments on earth-orbiting satellites, and these indicate that the growing season of vegetation and the frequency of natural disturbances have increased in response to climate change (Myneni *et al.* 1997; Nemani *et al.* 2003). Predictions of future changes in climate are uncertain, but it is very likely that they will be accelerated by continued and increasing emissions of CO_2 (IPCC 2007). Policy makers are seriously concerned that human-induced climate change is causing increasing risks of floods and droughts, and they need to be able to identify areas where these will occur. The risk of landslides and fires is also influenced by the type of vegetation present in any particular area.

At the broadest scale, we may need only to distinguish forests from other types of vegetation to evaluate the major hydrologic implications of differences in vegetative cover (Brown *et al.* 2008; Sun *et al.* 2006). We need more detail,

however, when millions of hectares of fertilized plantations of nonnative tree species are present on the landscape (Almeida and Soares 2003). To meet this challenge, models based on a fuller understanding of physiology, physics, and soil chemistry are required to predict the landscape-level hydrologic consequences.

Those of us interested in plant water relations recognize two main challenges that must be met to improve hydrologic models and apply them to landscapes (For areas larger than 50 hectares, the distribution of different types of vegetation, and their variations in albedo, aerodynamic conductance and access to water begin to interact with the local climate, which may require interactive land surface/atmospheric models to account for these effects if they cannot be monitored directly (Pielke *et al.* 1997, 1998).): first, we need to identify physiological principles that can be widely applied, and secondly, we need to relate those principles to attributes of vegetation that can be observed from space. If we succeed in meeting these objectives, future predictions of change will be more soundly based than at present and susceptible to global-scale verification (or falsification).

THE FACTORS LINKING VEGETATION WATER USE WITH ATMOSPHERIC CONDITIONS

The remote sensing community has long known that canopy LAI sets limits on evaporation and transpiration and that LAI can be estimated from differences in the reflection of wavebands in the visible and near-infrared (IR) part of the (electromagnetic) spectrum (Gates *et al.* 1965). The meteorological variables that drive evaporation from free water surfaces—the energy supplied by the sun and transfer processes driven by wind and vapor pressure deficits—including from wet leaves and transpiration, are also well understood and incorporated in the widely applied Penman–Monteith equation (Monteith 1965). This equation links those variables and land surface (plant canopy) properties through stomatal and canopy aerodynamic conductance.

The major constraints on evaporation from foliage are the amount of the surface that is wet and its aerodynamic conductance. In tall vegetation with small leaves, when the foliage is dry, transpiration is mainly constrained by canopy conductance (G), which is much smaller than the (high) aerodynamic conductance, even in still air. Canopy conductance is determined by LAI and stomatal conductance (g_s). The stomatal conductance of all leaves in the canopy is in parallel, so sums algebraically to give G . Shorter plants and trees with large leaves are less well coupled to the atmosphere because aerodynamic conductance is small. In these communities, if transpiration did not continue at an adequate rate, high radiation loads would quickly overheat the foliage, unless the amount of radiation intercepted can be reduced by wilting or leaf curling (Beerling *et al.* 2001).

The main variables that affect stomatal behavior are well known: leaf-to-air humidity deficits (D), water potential gradients ($\delta\psi$), which affect leaf turgor, light (photosynthetically active radiation [PAR]), leaf chemistry (N), temperature (T), and ambient CO_2 concentrations. In the field, most of these variables interact. In Fig. 1, data synthesized from measurements made in Amazonian rainforests are plotted to illustrate three interactions. With the exception of the first panel (PAR and D), the relationships between variables are nonlinear. Maximum canopy conductance (G_{max}) corresponds in this tropical forest to $T = 35^\circ\text{C}$, $D = 0.5$ kPa, and $\text{PAR} = 500$ W m^{-2} .

Mechanistic models have been developed to predict G , but the empirical model developed by Jarvis (1976) (Equation 1) often does as well or better (Lloyd *et al.* 1995; Whitley *et al.* 2009). The Jarvis model predicts g_s as a function of the maximum expected stomatal conductance ($g_{s\text{max}}$) constrained using nonlinear, multiplicative, independent variables that are normalized to range between 0 and 1 (As atmospheric concentrations of CO_2 rise, this function may exceed 1.0).

$$g_s = g_{s\text{max}} \cdot f(D) \cdot f(\delta\psi) \cdot f(\text{PAR}) \cdot f(N) \cdot f(T) \cdot f(\text{CO}_2) \quad (1)$$

The same formula has been applied to predict G (Kim *et al.* 2008, Novick *et al.* 2009; Oren *et al.* 1999). To do this, we substitute estimates of G_{max} for the $g_{s\text{max}}$ values appropriate to the various vegetation types with which we are concerned. Then, assuming that we can define the functional relationships

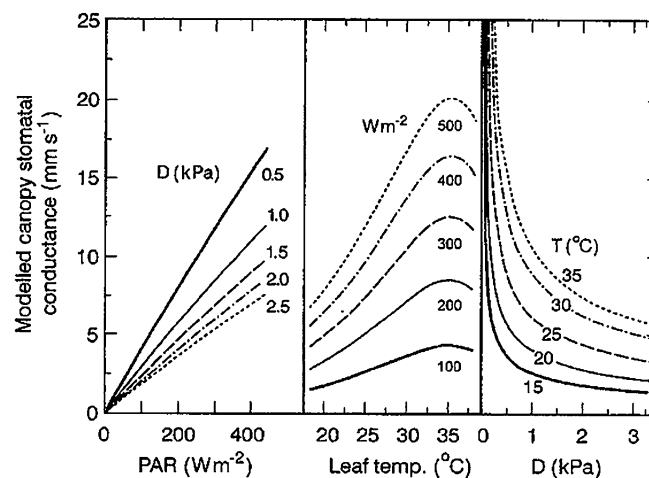


Figure 1: modeled data based on measurements of stomatal conductance made at an Amazonia rain forest site illustrate that canopy conductance (G) varies with meteorological conditions. G increases with photosynthetically active radiation (PAR), but less rapidly at higher values of D ; the increase with temperature (T) is much greater at high than at (relatively) low temperatures; decreases with vapor pressure gradient between the foliage and the air (D) are very rapid at all air temperatures, but note the differences in the rate of decline, and the lowest values reached, at different air temperatures. © 1995 by John Wiley and Sons, reprinted with permission, taken from Lloyd *et al.* (1995).

between g_s and the environmental factors that affect it, we calculate values of G to be used in the Penman–Monteith equation to estimate transpiration rates for those vegetation types. Given that we can estimate values for G_{\max} for an ecosystem or forest stand, the next step is to determine the functional relationships between G and the factors that affect it.

Clearly, the procedures and assumptions outlined in the previous paragraph are not trivial exercises. In the following sections, we provide examples of how G_{\max} has been estimated and how the functional relationships that constrain G_{\max} to give values for G have been generalized. In the final section of this paper, we discuss remote sensing techniques that have proven useful in scaling from processes at the level of trees and stands to ecosystems across landscapes—or seem likely to be useful and therefore warrant critical testing.

BIOPHYSICAL LIMITS ON MAXIMUM CANOPY CONDUCTANCE (G_{\max})

Effect of leaf–air vapor pressure deficits (D) on G

Work by Oren *et al.* (1999) and Sperry (2000) has made it very clear that stomata must act as the regulators of plant water potential and maintain it at values that can be sustained by the conducting system of the trees, that is, at values high enough to avoid catastrophic cavitation, when air enters the water conducting vessels and flow through them stops. So stomata will close when plants cannot sustain the rate of water loss driven by leaf–air vapor pressure deficit. The rate at which water can be supplied is affected by the capacity of the plant hydraulic system, including root–soil contact and the amount of water in the soil. As the vapor pressure deficit between leaf and air (D) increases, and supply rates fall behind demand, stomata respond by partial closure. G generally decreases exponentially as the evaporative demand increases. Given that other variables are optimum, Oren *et al.* (1999) showed that knowledge of g_{\max} was sufficient to describe the rate that leaf stomatal conductance (g_s) would be reduced. They established Equation (2):

$$g_s = g_{\max} - m \cdot \ln D \quad (2)$$

where m is the stomatal sensitivity and has a value of ~ 0.6 .

We can assume that G would respond similarly to D , but note that Equation (2) predicts that g_s goes to zero at moderate values of D , which is not, in fact the case (Landsberg and Sands 2011). We can also expect transpiration to reach a plateau during the day when G is not zero although D might increase by more than five-fold (Anthoni *et al.* 1999). There is also ample evidence (Waring and Franklin 1979) that, at low values of D , there is very little effect on stomatal conductance presumably because, at the low transpiration rates that result from those values, the supply of water to the foliage is fast enough not to impose any stress. Therefore, if there are no other limiting factors, $G \approx G_{\max}$. The main challenge in applying Equation (2) to canopies arises from the need to assume that canopy leaf temperature—which has a strong effect on D —is similar to

that of the ambient air. This will almost certainly be the case for rough canopies with small-leaved species, for which aerodynamic conductance will be high but may be a dubious assumption for canopies with large leaves, such as those that may be found in tropical forests.

Effect of water potential gradients ($\delta\psi$) on G

The discussion in the previous section implies that water potential gradients play a crucial role in determining canopy conductance. Reductions in canopy stomatal conductance are often correlated with reduction in surface soil water content because the large bulk of fine roots, which thoroughly permeate the soil, occur near the surface and those layers dry out rapidly. When they do so, high water potential gradients develop between the root absorbing surfaces and canopy foliage. Subsequent water extraction takes place from lower layers, but it is difficult to account for water uptake by roots that extend 10–25 m beneath the surface and can redistribute water in any direction depending on the water potential gradient (Amenu and Kumar 2007; Burgess *et al.* 2001). Even with shallow-rooted plants, the response of G to depletion in the water supply is highly dependent on soil texture (Bernier *et al.* 2002; Landsberg and Waring 1997). To predict how leaf and canopy conductance will respond to soil water deficits, it is often advisable to reference seasonal changes to $\delta\psi$ ($= \psi_{\text{spring}} - \psi_{\text{fall}}$) rather than to rely on monitoring soil water status (Running 1994). Meinzer *et al.* (1999) were able to derive a reasonable estimate of canopy conductance for a rainforest in Panama only when they accounted for differences in $\delta\psi$ among tree species and sizes of individuals.

It has long been assumed that the transpiration rate is zero in the early morning (predawn), so that foliage water potential (ψ_f) measured at that time is in equilibrium with soil water potential (ψ_s) (Waring and Cleary 1967). On this basis, it has been found that the relationship between predawn leaf water potential and midday values is a good predictor of maximum daytime leaf stomatal conductance (Fig. 2). However, we should note that if stomata do not close fully at night and transpiration continues, plant–soil water potential equilibration will not occur (Dawson *et al.* 2007; Kavanagh *et al.* 2007). Corrections can be applied as a function of D to estimate equilibrium predawn leaf water potential (Kavanagh *et al.* 2007).

Structural limitations

Canopy structure, i.e. tree height and crown width, may influence rates of water loss, through canopy conductance, in different directions (i.e. increase or decrease them). High LAI (up to about LAI ≈ 4 ; see Fig. 4) leads to increased water use, but tall trees increase water potential gradients and so tend to reduce G . The effects of canopy structure were dramatically illustrated by a 50% reduction in runoff when old-growth eucalyptus forests around Melbourne, Australia, were replaced, following fire, by dense stands of younger trees (Vertessy *et al.* 2001). The reductions were caused by greatly increased water use by the young re-growth, primarily

as a result of high LAI, but the fact that the trees were relatively short may also have contributed to higher values of g_s than those in tall old-growth trees, the combination leading to high values of G_{\max} and hence G . This is explained below.

The theoretical maximum tree height is between 125–130 m; most trees stop height growth below 40 m because suboptimal growing conditions create added resistance to water flow (Koch *et al.* 2004). The gravitational hydrostatic gradient is 0.01 MPa per meter. In redwood trees taller than 100 m, it accounts for two-third of the total resistance to water flow through the stems (Koch *et al.* 2004). This structural resistance to water flow increases with tree height because the vascular system becomes progressively less efficient as growth slows. These two resistances combine to reduce G_{\max} to a minimum that limits both photosynthesis and height growth (Brodribb and Feild 2000; Ryan and Yoder 1997). To establish how much differences in G_{\max} might be associated with height, Hubbard *et al.* (1999) compared 250-year-old ponderosa pine, 30 m high, with 40-year old trees 10 m high. They found that G_{\max} at mid-day, in the older trees, was ~30% less than in the younger trees.

On similar sites, open-grown trees are shorter than those growing in dense stands. This variation in height is associated with differences in the length of branches (Hubbard *et al.* 1999; Walcroft *et al.* 1996; Waring and Silvester 1994). To generalize the implications of variation in tree height and crown width requires knowledge of the potential tree height across a range of conditions, or alternatively, a correlation between height and crown growth rates and maximum tree height. Novick *et al.* (2009) examined the possibility that maximum canopy conductance may be proportional not only to the height of a tree but also to the ratio of leaf area per tree (A_F) to sapwood cross-sectional area (A_S). They derived a simple expression for

G_{\max} in terms of A_F , A_S , and tree height H that applied across 29 sites with a range of forest types, i.e.

$$g_{\text{Cref}} = 98.2 \frac{A_S}{A_F H} + 37.3. \quad (3)$$

This formula accounted for 75% of the variance in G_{\max} . Novick *et al.* (2009) found that there was only a weak general relationship between G_{\max} and height alone among 42 forested ecosystems, representing a large number of species from a wide range of climates, although there was a strong relationship when data from temperate sites were treated alone. We obviously need more work to establish the extent to which Equation (3), or some version of it, can be regarded as generally applicable to forest stands, but because forest height can be estimated from space, this approach clearly holds considerable promise (Landsberg and Sands 2011). The ratio A_F/A_S can be estimated from well-established relationships (Waring *et al.* 1982), so if we have estimates of LAI, and some information about tree populations, we can estimate A_F .

Effect of light (PAR) on G

As LAI increases, an increasing proportion of the leaves in the canopy is shaded by other leaves. The proportion changes depending on sun angle and the clarity (transmissivity) of the atmosphere. Under clear skies, the fraction of diffuse light is ~15%; under completely overcast conditions, it is 100%. Diffuse light casts no shadows and penetrates deeper into canopies than direct sunlight. There is now general acceptance that models designed to predict diurnal and daily trends in transpiration and photosynthesis should take into account the difference between sunlit and shaded components of the canopy (see the pioneering work Norman 1982 and, more recently, Bernier *et al.* 2001; Dai *et al.* 2003). These two-stream models synthesize knowledge of single-leaf physiology, and the physics of transpiration and the radiation regime within a canopy. They are valuable research tools that provide a biophysical basis for the responses of canopies to the various environmental and physiological factors that affect whole-canopy photosynthetic production and transpiration, but they are relatively complex and require detailed information about canopy structure (Landsberg and Sands 2011). However, there are simpler relationships that allow estimation of G : total light absorbed by the canopy tends to increase almost linearly up to an LAI of ~4.0 and then approaches a plateau (Fig. 3) and canopy conductance responds to increasing incident PAR in a similar nonlinear fashion (Baldochi and Hutchison 1986). Such relationships can be used to estimate $f(\text{PAR})$ in association with values of G_{\max} , to estimate G , although they need to be determined for a range of vegetation types.

Effects of nutrition on G

Estimates of G_{\max} have been made for a wide range of vegetation types growing under near optimum climatic conditions.

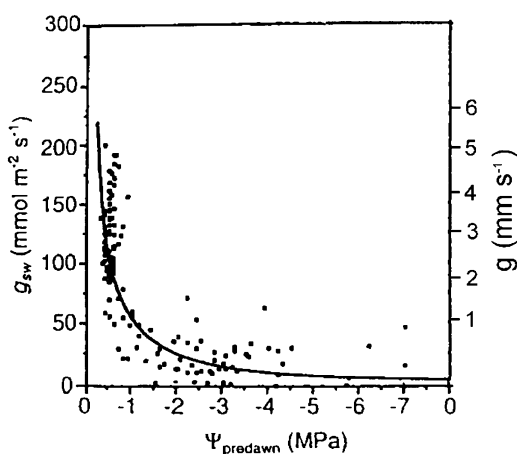


Figure 2: maximum daily stomatal conductance (g_s) of *Nothofagus solandri*, native New Zealand, shows an exponential decrease as predawn water potential falls. Two axes are provided for comparison of units. Molar units are currently more generally favored. © Oxford University Press, reprinted with permission, taken from Sun *et al.* (1995).

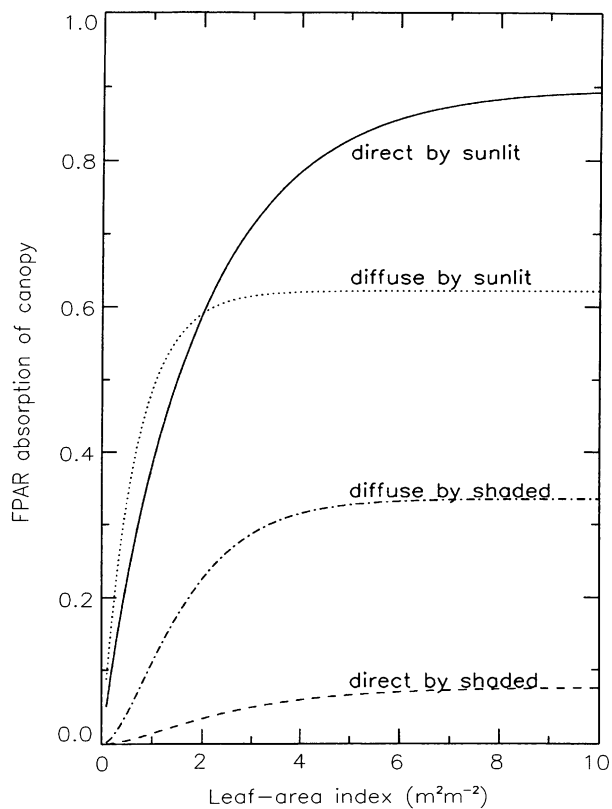


Figure 3: fraction of PAR absorbed by sunlit/shaded fractions of canopy for direct and diffuse incident PAR radiation, calculated with the sun directly overhead. © American Meteorological Society, reprinted with permission, taken from Dai *et al.* (2003).

Kelliher *et al.* (1995) reported G_{\max} (using units of m s^{-1}) (The following formula converts between these units and the molar units more commonly used nowadays; where $R = 8.314 \text{ J K}^{-1} \text{ mol}^{-1}$ is the universal gas constant, T ($^{\circ}\text{C}$) is the temperature and P (Pa) is the pressure. At 20°C at sea level, the conversion factor is $0.024 \text{ m}^3 \text{ mol}^{-1}$ (from Landsberg and Sands 2011).) values and standard errors for woody vegetation (16 studies) and natural herbaceous vegetation (5 studies) that averaged 0.02 ± 0.0015 and $0.017 \pm 0.0021 \text{ m s}^{-1}$, respectively, whereas the values for agricultural crops (9 studies) were significantly higher ($0.03 \pm 0.0035 \text{ m s}^{-1}$). Why the difference? The reason is that agricultural crops are generally well fertilized, whereas natural vegetation is not. In fertilized vegetation, the photosynthetic capacity (P_{\max}), which is strongly influenced by leaf nitrogen concentrations, and G_{\max} , are known to increase in parallel (Schulze *et al.* 1994, but see Evans 1989). This explains why photosynthetic capacity in fertilized plantations of young eucalyptus trees in Brazil may be more than double that of adjacent unfertilized rainforests (Almeida and Soares 2003). With less than half the LAI of the rainforests, the plantations transpire equivalent amounts of water because G_{\max} of the two types of vegetation is similar (Almeida and Soares 2003; but see Hubbard *et al.* 2004). This link between fN , P_{\max} , and G_{\max}

may be exploited with remote sensing, as we outline in a later section.

Effects of temperature (T) on G

For evergreen species, the optimum temperature (T_{opt}) for photosynthesis may shift by $>10^{\circ}\text{C}$ seasonally (Hember *et al.* 2010; Slatyer and Morrow 1977; Strain *et al.* 1976). Mean daytime air temperatures often correspond to seasonal T_{opt} , as indicated in Fig. 4. It is worth noting that the current climate in which a species grows may not correspond to its optimum temperature. In New Zealand, many of the native tree species are adapted to ambient temperatures 10°C warmer than now observed (Hawkins and Sweet 1989). Way and Oren (2010) suggest that climatic warming may benefit boreal forest species but impose limitations on tropical vegetation if temperatures exceed T_{opt} (e.g. $>35^{\circ}\text{C}$ in Fig. 1). Minimum temperatures are also important if they drop below -2°C causing stomatal closure that may persist for some days (Hadley 2000; Running *et al.* 1975; Smith *et al.* 1984).

Effect of CO_2 on G

The dependence of g_s on CO_2 ($f\text{CO}_2$) in Equation 1) arises from the fact that trees, and other plants with C_3 biochemical photosynthetic pathway, can reduce carbon dioxide concentration inside mesophyll cells to $\sim 70\%$ of that of ambient air. There is some argument about whether the parallel responses of assimilation and conductance reflect responses of stomata to intercellular CO_2 concentrations, or simply parallel responses to light (Morison and Jarvis 1983), but there is strong evidence that stomata of broadleaf trees are responsive to high CO_2 , whereas those of conifers are not (Brodribb *et al.* 2009).

In the C_3 plants responsive to variations in ambient air CO_2 concentrations, increases in these concentrations may cause reduced stomatal conductance, and hence reduced canopy conductance, while permitting photosynthesis to increase (Fig. 5). As a result, water use efficiency increases. In areas where water limits canopy development, LAI would be expected to increase with rising concentrations of ambient CO_2 (Macinnis-Ng *et al.* 2010). This response is contingent on an adequate supply of nutrients to support additional LAI (Finzi *et al.* 2008; Lloyd 1999). A rise in atmospheric CO_2 may partly compensate for higher D (Equation 1, Fig. 1). The implications of this effect, in relation to the water and energy balance of ecological communities, were explored by Field (1983).

THE ROLE OF MODELS

We started this paper by introducing a simple model that includes the major variables controlling G and progressed to describe the (usually nonlinear) relationships associated with each term. Although we might be able to discover remote sensing techniques that can define above-ground properties of the vegetation and surface soil/litter, none will

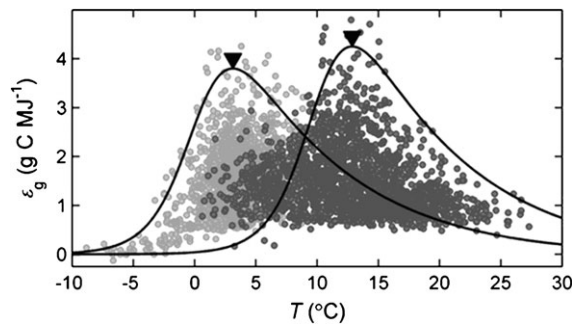


Figure 4: optimum temperature for rates of gross photosynthesis (ϵ_g) varies seasonally by 10°C between November and March (light gray points) and April through September (dark gray points), for coastal Douglas-fir. Inverted triangles correspond to mean daytime temperatures for the two periods. © Elsevier, reprinted with permission, taken from Hember *et al.* (2010).

directly measure those below ground that affect leaf nutrition and plant water relations. Where G might be constrained by drought or nutrition, model sensitivity analyses that predict daily transpiration, combined with LAI observations, can provide indirect estimates of water storage capacity in root zones (Ichii *et al.* 2007; Kleidon and Heimann 1998) and of soil fertility (Stape *et al.* 2006). The success of this modeling approach often depends on whether LAI values are less than or $>4.0 \text{ m}^2 \text{ m}^{-2}$. At the higher values where, as shown in Fig. 3, light absorbed by the canopy reaches a plateau, the application of techniques that depend on the differential-absorbance or reflectance properties of leaves, across different wave-band intervals, is limited. (This is discussed in the next section.)

We recognize that some hydrologic models do quite well—predicting seasonal and interannual patterns of stream flow, drought, and floods without detailed knowledge of the state of current vegetation. This is particularly true where winter snowpack is highly variable and reservoirs store runoff for large-scale irrigation projects during the growing season (Hamlet and Lettenmaier 1999). In such cases, plant–water relations play a minor role and the major requirements for predictions of catchment water use and water yields—a function of runoff—are weather data and good topographic and vegetation maps. In other cases, where the vegetation plays a more dominant role in catchment hydrology, biophysical process-based models have improved forecasts and help to explain interactions and options for management (e.g. Cox *et al.* 1998; Chen *et al.* 2005; Schultz 1996; Soares and Almeida 2001; Feikema *et al.* 2010).

Application of remote sensing

A number of the variables about which we need information to initialize and drive landscape-level hydrologic models can now be measured by satellite-borne sensors. Table 1 provides a summary of those for which values can be obtained and indicates

the types of sensors that can provide the relevant data. These sensors are mounted on a variety of satellites.

Based on our understanding of the hydrologic cycle, plant physiology and physics, we can list the kinds of data needed to generalize plant–water relations to landscapes. First, a digital elevation map will be required to define drainage basins, to account for topographic variation in climate and soils and to map variations in type and structure of vegetative cover. Secondly, we need to distinguish whether evaporative surfaces are wet or dry. Thirdly, we require climatic data on daytime vapor pressure deficit, incident solar radiation (of which $\sim 50\%$ is PAR), temperature, precipitation and progressive changes in atmospheric CO_2 concentrations.

The most important properties of the vegetation include seasonal and interannual variation in LAI, both horizontally and vertically. Also, assessment of photosynthetic capacity (P_{max}) is required to take into account the effects of nutritional variation, and serve as a surrogate for G_{max} . In drought-prone areas, vegetation that has access to deep sources of water will need to be distinguished from that with limited access.

In the sections below, we separate our presentation into two broad categories: climatic variables that drive transpiration and evaporation and biological variables that constrain the rates that water is lost.

Remotely sensed climatic drivers

At present, most climatic variables required to drive the Penman-Monteith equation, as well as parameterize Equation 1, can be obtained at daily resolutions (or better) from a range of weather satellites. Over the past three decades, various approaches have been developed to predict incident short-wave radiation and PAR from satellite-derived data (Eck and Dye 1999; Pinker and Laszlo 1992). Goward *et al.* (1994) and Dye and Shibasaki (1995) estimated monthly integrated incident solar radiation using ultraviolet reflectance from the Total Ozone Mapping Spectroradiometer. Wang *et al.* (2000) combined finer scale Landsat imagery, a digital elevation model, and an atmospheric transmission model (LOWTRAN) to estimate surface net solar radiation over an agricultural site in the United States with an average error of $<\text{less than } 1\%$. More recently Liang *et al.* (2006) produced accurate daily estimates of incident solar radiation and PAR at a spatial resolution of 1 km^2 or less by combining information from a number of satellite sensors.

Surface estimates of vapor pressure deficits can also be retrieved at a similar resolution to PAR with good results up to D of 2.5 kPa using land surface temperature (LST) data acquired by the Moderate Resolution Imaging Spectroradiometer sensor on National Aeronautics and Space Administration's (NASA's) Terra and Aqua satellites, except where vegetation is very sparse (Hashimoto *et al.* 2008; Nemani 2008). On overcast days, when surface temperatures cannot be retrieved, it is unlikely the D will be suboptimal. Frozen soils can be detected with RADAR to define conditions when stomata are closed and growth cannot occur (Kimball *et al.* 2004). On clear days,

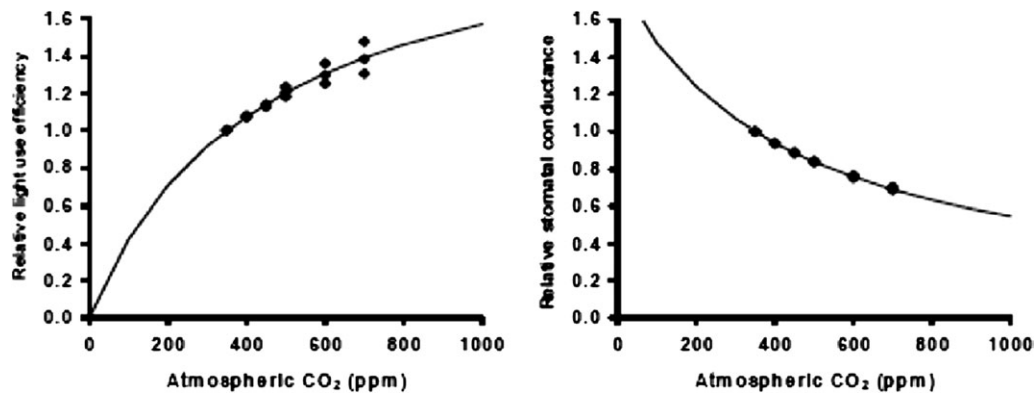


Figure 5: modeled relationship light-use efficiency (left) and relative leaf stomatal conductance (g_s) (right) with ambient CO_2 concentrations. © The Modeling and Simulation Society of Australia and New Zealand Inc., with permission, taken from Almeida *et al.* (2009).

Table 1: remotely sensed surface properties of landscapes to scale plant–water relations

Variables	Value	Sensors
LAI	Recognize drought, set limits on transpiration	Visible and near IR
Vegetation type and disturbance	Classify vegetation and record disturbance and recovery	Thermal IR, visible, and near IR
Surface dryness	Index of surface soil moisture and canopy wetness	Thermal IR, visible, and near IR, Radar
Freeze-thaw temperature	Define growing season in cold climates and limits G	Radar
Flooded conditions under vegetation	Recognize flooding under cloud cover	Radar
Photosynthetic capacity and max canopy conductance	Defines P_{\max} , G_{\max} and response to D	Hyperspectral (absorbed PAR by chlorophyll)
Stomatal closure in dense forest	Confirm modeled estimates of soil water depletion	Hyperspectral (PRI)
Height of vegetation	Account for hydraulic resistance in stems	Lidar, radar
Crown width	Account for hydraulic resistance in branches	High spatial resolution, visible (1 m), Lidar

LST can be estimated and compared with values extrapolated from a variety of sources.

Precipitation is the most difficult climatic variable to acquire remotely and consistently across large areas. As a result most process-based models utilize ground networks of precipitation extrapolated across space and time. However, progress is being made using a combination of passive microwave sensors (Nesbitt *et al.* 2004) with a number of new satellite missions planned to resolve this data gap.

Remotely sensed features of vegetation

Structural features.

The area occupied by different types of vegetation can be mapped based on differences in seasonal patterns of LAI, recognized by variation in reflectance patterns in the visible, near-IR, and thermal IR measurements of LST (Running *et al.* 1995). The height of trees as well as crown widths can be monitored with both passive and active sensors. SPOT (Satellite Pour l'Observation de la Terre) coverage in the visible and near IR at 1-m spatial resolution is generally adequate to define crown widths (Cohen and Spies 1992). Active sensors

such as radar and Lidar, which send out pulses and monitor the strength of their return, provide good measures of tree heights and the distribution of LAI vertically and horizontally (Fig. 6), as well as individual crown width (Popescu *et al.* 2003). Together, interferometric radar and Lidar offer opportunities to characterize much larger areas, although with less accuracy that might be attained from airborne Lidar (Neeff *et al.* 2005; Treuhaft *et al.* 2009). Much can be gained by assembling data from a number of different remote sensing sources and using geographic information systems to display the results (see review by Fargan and Defries 2009).

Remotely sensing indices of drought.

For broad-scale geographic analyses, the remote sensing community has generally relied on drought indices that do not involve calculation of a soil water balance (e.g. Zhao and Running 2010). Drought-prone areas can be recognized, and reasonable values of LAI (and Normalized Difference Vegetation Index (NDVI)) can be generated by modeling, using a range of soil water storage capacities. At the other extreme, flooded areas, even those covered by dense forests, are easily

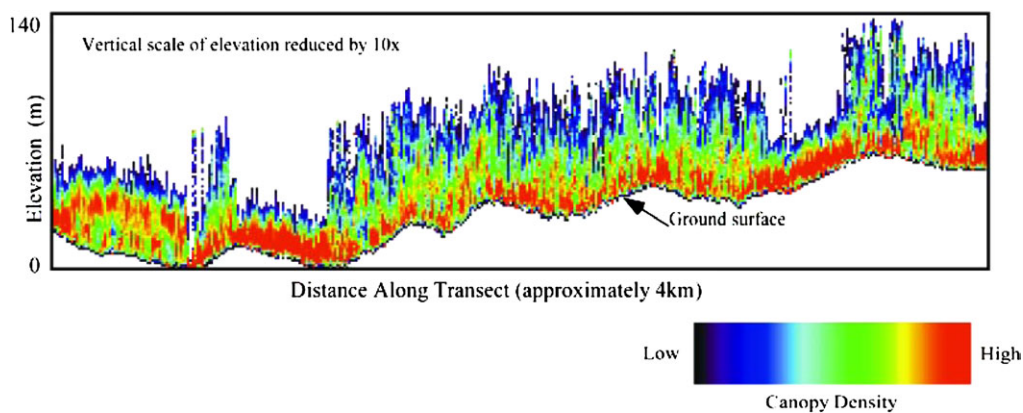


Figure 6: measurements of canopy structure made using Lidar (National Aeronautics and Space Administration's Scanning Lidar Imager of Canopies by Echo Recovery). Panel (a) shows ground topography and the vertical distribution of canopy material along a 4-km transect in the H. J. Andrews Experimental Forest, Oregon. Modified from Fig. 3 in Lefsky *et al.* (2002).

recognized by the intense backscatter signal from RADAR (Waring *et al.* 1995).

To date, the most widely applied remotely sensed index of drought involves an analysis of landscape-level changes in the relationship between NDVI and the integrated canopy and LST, T_s (Nemani and Running 1989). As previously noted, the canopies of tall, dense forests tend to remain near ambient air temperature whether transpiration continues or stops. In a landscape containing vegetation with a range in LAI, a vegetation greenness index (NDVI IR to red reflectance) can be used in combination with T_s measurements to infer progressive depletion of surface soil water supply by observing an increase in the slope in the relationship depicted in Fig. 7. Precipitation that wets all surfaces results in similar temperatures across the full range in NDVI.

The relationship between NDVI and T_s is not a direct measure of plant water stress. Measuring a reduction in the water content of foliage would offer a more direct correlate with water stress and its influence on G . Much effort has been expended to use, for this purpose, subtle differences in reflectance of narrow near-IR spectral bands that are associated with change in water content as well as with narrow spectral bands in visible wavelengths caused by changes in anthocyanin pigments that reflect stress. Forests with dense canopies should be ideal for using fine-resolution spectral reflectance to sense drought, and where experiments have been conducted to create drought by redistributing precipitation off a site, the results are impressive (Fig. 8). In tropical forests, however, where new foliage is produced at the top of the canopy before the wet season begins, this may result in changes in the near IR reflectance that confound analyses (Asner and Alencar 2010). In addition, all fine-resolution spectral reflectance analyses derived from satellite-borne sensors must correct for seasonal and spatial variation in the amount of water vapor, haze, and smoke, as well as changes in viewing angle (Asner and Alencar 2010).

Remotely sensed indicators nutrition: photosynthetic capacity and efficiency

Initially, the aim of most measurements made by remote sensing, with the objective of predicting hydrologic responses to climatic variation, was to provide data for models that applied to broadly defined types of vegetation—or biomes—in which it was assumed that a relationship exists between canopy greenness (LAI), photosynthetic capacity (P_{\max}) and G_{\max} (Sellers *et al.* 1992). Within similar types of vegetation, considerable variation in LAI and P_{\max} was recognized and often related to differences in leaf chemistry, in particular, total nitrogen content (Pierce *et al.* 1994). For evergreen needle-leaf species, total nitrogen in the canopy increases linearly with a 10-fold change in LAI, although nitrogen per unit of leaf area decreased by 3-fold (Pierce *et al.* 1994). This reflects a corresponding change in leaf structure (mass per unit area) that can affect the overall reflectance properties (albedo). Differences in albedo can be remotely sensed and, thus, have been used as a surrogate for nitrogen and P_{\max} (Ollinger *et al.* 2008). Smith *et al.* (2002) were among the first to use fine-resolution (hyperspectral) spectrometry acquired in the near-IR part of the spectrum from aircraft, to measure nitrogen content in foliage of mixed, temperate forests, and link this to P_{\max} .

Although P_{\max} tends to increase with foliar nitrogen content, the relation is not always linear. The photosynthetic capacity of leaves is related to the nitrogen content because the photosynthetic machinery and process (thylakoids and enzymes in the Calvin cycle) represent the majority of leaf nitrogen (Evans 1989). At very high levels of nitrogen, the proportion in soluble protein increases without any effect on photosynthesis. Evans (1989) suggests that chlorophyll content would be a better measure of P_{\max} than total N because thylakoid nitrogen is directly proportional to the chlorophyll content. Zhang *et al.* (2005, 2009) took advantage of this relationship using hyperspectral remote sensing of the sunlit (most active) portions of forest canopies to assess chlorophyll

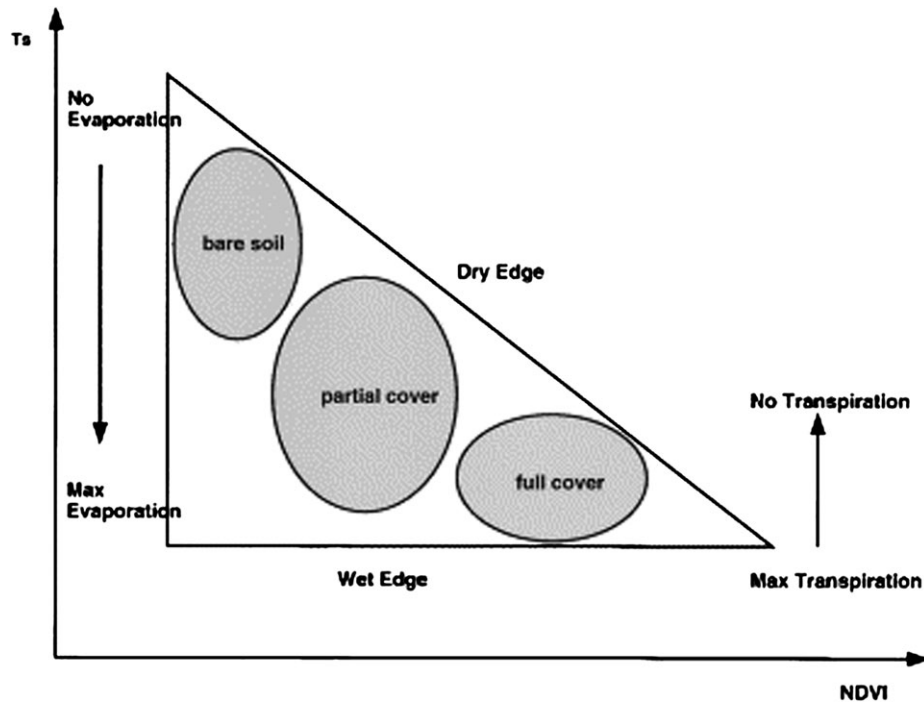


Figure 7: As the surface dries, land-surface temperatures (T_s) rise to higher values on exposed soils than under full plant cover, recognized by the maximum value of the NDVI, a surrogate for LAI. These two remotely sensed variables can be combined into a vegetation dryness index that correlates with depletion of water from surface soils. Seasonal variation in ambient air temperature, which is similar to canopy leaf temperatures of tall, dense needle-leaf forests, can be estimated by extrapolating T_s to maximum values of NDVI. © Elsevier, reprinted with permission, taken from Sandholt *et al.* (2002).

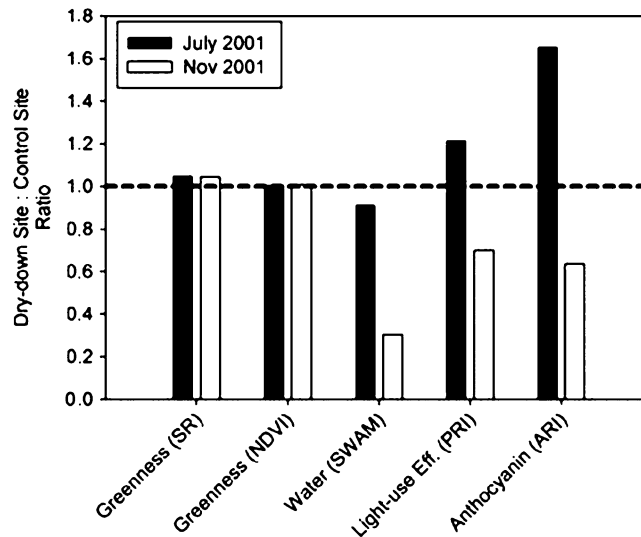


Figure 8: seasonal variation in water stress (July low, November high) in an Amazon tropical forest shows little change in broad-band reflectance indices between drought and nondrought conditions, e.g. simple ratio (SR) of near IR to red (R) reflectance or the NDVI = (near IR - R)/(near IR + R). Narrow-band reflectance indices for water (SWAM), photosynthetic light-use efficiency (PRI) and anthocyanin pigments (ARI). Copyright (2004) National Academy of Sciences, USA., reprinted with permission, taken from Asner *et al.* (2004).

content and correlate that with measured P_{max} . Through remotely sensed measurement of canopy chlorophyll content, we might, therefore, obtain an indirect estimate of G_{max} .

Chlorophyll (a and b) are very stable pigments; others are less stable under conditions when photosynthesis is downregulated. Gamon *et al.* (1992) noted that a shift in the

composition of xanthophyll pigments occurs when stomata begin to close, which results in a change in reflectance at 531 nm relative to chlorophyll reflectance at 730 nm. This shift in the ratio of reflectance from different forms of xanthophyll pigments is defined as the photosynthetic reflectance index (PRI). It is known to vary hourly and seasonally (Hall *et al.* 2008; Hember *et al.* 2010). Where other measures of canopy water stress can be inferred by modeling or through other hyperspectral stress indices (Fig. 8). PRI warrants testing as a surrogate for both G_{\max} and G . The challenges to obtaining precise estimates of PRI, and other hyperspectral indices, are many, but progress is being made (Drolet *et al.* 2008; Hilker *et al.* 2009).

CONCLUDING REMARKS

The central point that we have been making throughout this paper is that, given information about the canopy structure of vegetation, and adequate weather data—among which precipitation amounts and patterns are probably the most important variables—we can estimate water use with considerable accuracy with a series of landscape-linked models. Within the Penman–Monteith equation, the canopy conductance (G) term describes the interaction between canopies and the atmospheric environment, so our ability to derive accurate values for that term is central to our ability to estimate transpiration rates by ecosystems. Equation (1) encapsulates the factors that we know determine G and much of our discussion has been concerned with those factors and their effects. The height and crown width of plants do not require frequent monitoring, but it is critical to document seasonal variation in LAI. The chlorophyll content of sunlit foliage, which is correlated with P_{\max} , and in turn G_{\max} is needed to predict the response of G to D (Equation 2). In arid environments, a series of hyperspectral indices (SWAM, PRI, ARI; Fig. 8) warrant testing as to their reliability in representing water stress induced by drought, particularly where LAI values remain stable, along with more general remotely sensed indices (SR and NDVI). Asbjornsen *et al.* (2011) provide a more complete review on this subject in regard to other methods available to interpret the effects of vegetation on landscape hydrology.

FUNDING

U.S. National Aeronautics and Space Administration (grant no. NNX09AR59G to R.H.W.) from the Biodiversity and Ecological Forecasting Program.

ACKNOWLEDGEMENTS

We appreciate the invitation from Jiquan Chen and Huilin Gao to prepare a paper for this special issue of the journal. The paper contains some information on remote sensing technologies that was extracted from a longer review article on predicting the growth of forests with models and remotely sensed measurements (Waring *et al.* 2010).

Conflict of interest statement. None declared.

REFERENCES

- Almeida AC, Sands PJ, Bruce J, *et al.* (2009) Use of a spatial process-based model to quantify forest plantation productivity and water use efficiency under climate change scenarios. *18th World IMACS/MODSIM Congress, Cairns, Australia, 13–17 July 2009*, p. 1816–22. <http://mssanz.org.au/modsim09> (25 January 2011, date last accessed).
- Almeida AC, Soares JV (2003) Comparação entre o uso de água em plantações de *Eucalyptus grandise* floresta ombrófila densa (Mata Atlântica) na costa leste do Brasil. (Comparison of water use by *Eucalyptus grandis* plantations and Atlantic rainforest near the eastern coast of Brazil). *Revista Árvore* **27**:159–70.
- Amenun GG, Kumar P (2007) A model for hydraulic redistribution incorporating coupled soil-root moisture transport. *Hydrol Earth Syst Sci Discuss* **4**:3719–69.
- Anthoni PM, Law BE, Unsworth MH (1999) Carbon and water vapor exchange of an open-canopied ponderosa pine ecosystem. *Agric For Meteorol* **95**:151–68.
- Asbjornsen H, Goldsmith GR, Alvarado-Barrientos MS, *et al.* (2011) Ecohydrological advances and applications in plant-water relations research: a review. *J Plant Ecol* **4**:3–22.
- Asner GP, Alencar A (2010) Drought impacts on the Amazon forest: the remote sensing perspective. *New Phytol* **187**:569–78.
- Asner GP, Nepstad D, Cardinot G, *et al.* (2004) Drought stress and carbon uptake in an Amazon forest measured with spaceborne imaging spectroscopy. *Proc Natl Acad Sci U S A* **101**:6039–44.
- Baldocchi DD, Hutchison BA (1986) On estimating canopy photosynthesis and stomatal conductance in a deciduous forest with clumped foliage. *Tree Physiol* **2**:155–68.
- Beerling DJ, Osborne CP, Chaloner WG (2001) Evolution of leaf-form in land plants linked to atmospheric CO₂ decline in the late Palaeozoic era. *Nature* **410**:352–4.
- Bernier PY, Bréda N, Granier A, *et al.* (2002) Validation of a canopy gas exchange model and derivation of a soil water modifier for transpiration for sugar maple (*Acer saccharum* Marsh.) using sap flow density measurements. *For Ecol Manage* **163**:185–96.
- Bernier PY, Raulier F, Stenberg P, *et al.* (2001) Importance of needle age and shoot structure on canopy photosynthesis of balsam fir (*Abies balsamea*): a spatially inexplicit modeling analysis. *Tree Physiol* **21**:815–30.
- Brodribb TJ, Feild TS (2000) Stem hydraulic supply is linked to leaf photosynthetic capacity: evidence from New Caledonian and Tasmanian rainforests. *Plant Cell Environ* **23**:1381–8.
- Brodribb TJ, McAdam SAM, Jordan GJ, *et al.* (2009) Evolution of stomatal responsiveness to CO₂ and optimization of water-use efficiency among land plants. *New Phytol* **183**:839–47.
- Brown TC, Hobbins MT, Ramirez JA (2008) Spatial distribution of water supply in the conterminous United States. *J Am Water Res Assoc* **44**:1474–87.
- Burgess SSO, Adams MA, Turner NC, *et al.* (2001) Tree roots: conduits for deep recharge of soil water. *Oecologia* **126**:158–65.
- Chen JM, Chen X, Ju W, *et al.* (2005) Distributed hydrological model for mapping evapotranspiration using remote sensing inputs. *J Hydrol* **305**:15–39.
- Cohen WB, Spies TA (1992) Estimating structural attributes of Douglas-fir/western hemlock forest stands from Landsat and SPOT imagery. *Remote Sens Environ* **41**:1–17.

- Cox PM, C. Huntingford C, *et al.* (1998) A canopy conductance and photosynthesis model for use in a GCM land surface scheme. *J Hydrol* **212–213**:79–94.
- Dai Y, Dickinson RE, Wang Y-P (2003) A two big-leaf model for canopy temperature, photosynthesis, and stomatal conductance. *J Climate* **17**:2281–99.
- Dawson TD, Burgess SSO, Tu KP, *et al.* (2007) Nighttime transpiration in woody plants from contrasting ecosystems. *Tree Physiol* **27**:561–75.
- Drolet GG, Middleton EM, Huemmrich KF, *et al.* (2008) Regional mapping of gross light-use efficiency using MODIS spectral indices. *Remote Sens Environ* **112**:3065–78.
- Dye D, Shibasaki R (1995) Intercomparison of global PAR data sets. *Geophys Res Lett* **22**:2013–6.
- Eck TF, Dye DG (1999) Satellite estimation of incident photosynthetically active radiation using ultraviolet reflectance. *Remote Sens Environ* **38**:135–46.
- Evans J (1989) Photosynthesis and nitrogen relationships in leaves of C₃ plants. *Oecologia* **78**:9–19.
- Fargan M, Defries R (2009) Measuring and monitoring the world's forests: a review and summary of remote sensing technical capabilities 2009–2015. *Resour Future*, Washington, D.C. http://www.rff.org/rff/documents/rff-rpt-technical%20capacity_macauley%20et%20al.pdf (27 January 2011, date last accessed).
- Feikema PM, Morris JD, Beverly CR, *et al.* (2010) Validation of plantation transpiration in south-eastern Australia estimated using the 3PG+ forest growth model. *For Ecol Manage* **260**:663–78.
- Field C (1983) Allocating leaf nitrogen for the maximization of carbon gain: Leaf age as a control on the allocation program. *Oecologia* **56**:341–7.
- Finzi AC, Moore DJP, DeLucia EH, *et al.* (2008) Progressive nitrogen limitation of ecosystem processes under elevated CO₂ in a warm-temperate forest. *Ecology* **87**:15–25.
- Gamon JA, Peñuelas J, Field CB (1992) A narrow-waveband spectral index that tracks diurnal changes in photosynthetic efficiency. *Remote Sens Environ* **41**:35–44.
- Gates DM, Keegan HJ, Schleter JC, *et al.* (1965) Spectral properties of plants. *Appl Optics* **4**:11–20.
- Goward SN, Waring RH, Dye DG, *et al.* (1994) Ecological remote sensing at OTTER: satellite macroscale observations. *Ecol Appl* **4**:322–43.
- Hadley JL (2000) Effect of daily minimum temperature on photosynthesis in eastern hemlock (*Tsuga canadensis* L.) in autumn and winter. *Arctic Antarctic Alpine Res* **32**:368–74.
- Hall FG, Hilker T, Coops NC, *et al.* (2008) Multi-angle remote sensing of forest light use efficiency by observing PRI variation with canopy shadow fraction. *Remote Sens Environ* **112**:3201–11.
- Hamlet AF, Lettenmaier DP (1999) Effects of climate change on hydrology and water resources in the Columbia River Basin. *J Am Water Resour Assoc* **35**:1597–673.
- Hashimoto H, Dungan JL, White MA, *et al.* (2008) Satellite-based estimation of surface vapor pressure deficits using MODIS land surface temperature data. *Remote Sens Environ* **112**:142–55.
- Hawkins BJ, Sweet GB (1989) Photosynthesis and growth of present New Zealand forest trees relate to ancient climates. *Ann. Sci. For.* **46**:512s–514s.
- Hember RA, Coops NC, Black TA, *et al.* (2010) Simulating gross primary production across a chronosequence of coastal Douglas-fir stands with a production efficiency model. *Agric For Meteorol* **150**:238–53.
- Hilker T, Lyapustin A, Hall FG, *et al.* (2009) An assessment of photosynthetic light use efficiency from space: modeling the atmospheric and directional impacts on PRI reflectance. *Remote Sens Environ* **113**:2463–75.
- Hubbard RM, Bond BJ, Ryan MG (1999) Evidence that hydraulic conductance limits photosynthesis in old ponderosa pine trees. *Tree Physiol* **19**:165–72.
- Hubbard RM, Ryan MG, Giardin CP, *et al.* (2004) The effect of fertilization on sap flux and canopy conductance in a *Eucalyptus saligna* experimental forest. *Global Change Biol* **10**:427–36.
- Ichii K, Hashimoto H, White MA, *et al.* (2007) Constraining rooting depths in tropical rainforests using satellite data and ecosystem modeling for accurate simulation of gross primary production seasonality. *Global Change Biol* **13**:67–77.
- IPCC Summary for policymakers. *Climate Change 2007: The Physical Science Basis. Contribution of Working Group I to the Fourth Assessment Report of the Intergovernmental Panel on Climate Change*. Cambridge, UK: Cambridge University Press.
- Jarvis PG (1976) The interpretation of the variation in leaf water potential and stomatal conductance found in canopies in the field. *Philos. Trans. R. Soc. Lond. B Biol. Sci.* **273**:593–610.
- Kavanagh KL, Pangle R, Schotzko AD (2007) Nocturnal transpiration causing disequilibrium between soil and stem predawn water potential in mixed conifer forests of Idaho. *Tree Physiol* **27**:621–9.
- Kelliher FM, Leuning R, Raupach MR, *et al.* (1995) Maximum conductances for evaporation from global vegetation types. *Agric. For. Meteorol.* **73**:1–16.
- Kim H-S, Oren R, Hinckley TM (2008) Actual and potential transpiration and carbon assimilation in an irrigated poplar plantation. *Tree Physiol* **28**:559–77.
- Kimball JS, McDonald KC, Running SW, *et al.* (2004) Satellite radar remote sensing of seasonal growing seasons for boreal and subalpine evergreen forests. *Remote Sens Environ* **90**:243–58.
- Kleidon A, Heimann M (1998) A method of determining rooting depth from a terrestrial biosphere model and its impacts on the global water and carbon cycle. *Global Change Biol* **4**:275–86.
- Koch GW, Sillett SC, Jennings GM, *et al.* (2004) The limits to tree height. *Nature* **428**:851–4.
- Landsberg JJ, Sands PJ (2011) *Physiological Ecology of Forest Production: Principles, Processes and Modelling*. Oxford, UK: Elsevier Inc.
- Landsberg JJ, Waring RH (1997) A generalised model of forest productivity using simplified concepts of radiation-use efficiency, carbon balance and partitioning. *For Ecol Manage* **95**:209–28.
- Liang S, Zheng T, Liu R, *et al.* (2006) Estimation of incident photosynthetically active radiation from Moderate Resolution Imaging Spectrometer data. *J Geophys Res* **111**:D15208.
- Lefsky MA, Cohen WB, Parker GG, *et al.* (2002) Lidar remote sensing for ecosystem studies. *BioScience* **52**:19–30.
- Lloyd J (1999) The CO₂ dependence of photosynthesis, plant growth responses to elevated CO₂ concentrations and their interaction with soil nutrient status, II. Temperate and boreal forest productivity and the combined effects of increasing CO₂ concentrations and increased nitrogen deposition at a global scale. *Funct Ecol* **13**:439–59.

- Lloyd J, Grace J, Miranda AC, *et al.* (1995) A simple calibrated model of Amazon rainforest productivity based on leaf biochemical properties. *Plant Cell Environ* **18**:1129–45.
- Macinnis-Ng C, Zeppel M, Williams M, Eamus D (2010) Applying a SPA model to examine the impact of climate change on GPP of open woodlands and the potential for woody thickening. *Ecohydrology* .
- Meinzer FC, Andrade JL, Goldstein G, *et al.* (1999) Partitioning of soil water among canopy trees in a seasonally dry tropical forest. *Oecologia* **121**:293–301.
- Monteith JL (1965) Evaporation and environment. *Symp Soc Exp Biol* **29**:205–34.
- Morison JIL, Jarvis PG (1983) Direct and indirect effects of light on stomata. II In *Commelina communis* L. *Plant Cell Environ* **6**:103–9.
- Myneni RB, Keeling CD, Tucker GJ, *et al.* (1997) Increased plant growth in the northern high latitudes from 1981 to 1991. *Science* **386**:698–702.
- Neeff T, Dutra LV, dos Santos JR, *et al.* (2005) Tropical forest measurement by interferometric height modeling and P- band radar backscatter. *Forest Sci* **51**:585–94.
- Nemani RR (2008) Satellite-based estimation of surface vapor pressure deficits using MODIS land surface temperature data. *Remote Sens Environ* **112**:142–55.
- Nemani RR, Keeling CD, Hashimoto H, *et al.* (2003) Climate-driven increases in global terrestrial net primary production from 1982 to 1999. *Science* **300**:1560–3.
- Nemani RR, Running SW (1989) Estimation of regional surface resistance to evapotranspiration from NDVI and thermal-IR AVHRR data. *J Appl Meteorol* **28**:276–84.
- Nesbitt SW, Zipser EJ, Kummerow CD (2004) An examination of Version-5rainfall estimates from the TRMM Microwave Imager, precipitation radar, andrain gauges on global, regional, and storm scales. *J Appl Meteorol* **43**:1016–36.
- Norman JM (1982) Simulation of microclimate. In: Hadtfield JL, Thompson IJ (eds). *Biometeorology in Integrated Pest Management*. New York: Academic Press.
- Novick K, Oren R, Stoy P, *et al.* (2009) The relationship between reference canopy conductance and simplified hydraulic architecture. *Adv Water Resour* **32**:809–19.
- Ollinger SV, Richardson AD, Martin ME, *et al.* (2008) Canopy nitrogen, carbon assimilation, and albedo in temperate and boreal forests: functional relations and potential climate feedbacks. *Proc Natl Acad Sci USA* **105**:19335–40.
- Oren R, Sperry JS, Katul GG, *et al.* (1999) Survey and synthesis of intra-and interspecific variation in stomatal sensitivity to vapour pressure deficit. *Plant Cell Environ* **22**:1515–26.
- Pielke RA Sr, Avissar R, Raupach M, *et al.* (1998) Interactions between the atmosphere and terrestrial ecosystems: influence on weather and climate. *Global Change Biol* **4**:461–75.
- Pielke RA Sr, Lee TJ, Copeland JH, *et al.* (1997) Use of USGS-provided data to improve weather and climate simulations. *Ecol Appl* **7**:3–21.
- Pierce LL, Running SW, Walker J (1994) Regional-scale relationships of leaf area index to specific leaf area and leaf nitrogen content. *Ecol Appl* **4**:313–21.
- Pinker RT, Laszlo I (1992) Modeling surface solar irradiance for satellite applications on a global scale. *J Appl Meteorol* **31**:194–211.
- Popescu SC, Wynne RH, Nelson RF (2003) Measuring individual tree crown diameter with LiDAR and assessing its influence on estimating forest volume and biomass. *Can J Remote Sens* **29**:564–77.
- Running SW (1994) Testing forest-BGC ecosystem process simulations across a climatic gradient in Oregon. *Ecol Appl* **4**:238–47.
- Running SW, Loveland T, Pierce L, *et al.* (1995) A remote sensing based vegetation classification logic for global land cover analysis. *Remote Sens Environ* **51**:39–48.
- Running SW, Waring RH, Rydell RA (1975) Physiological control of water flux in conifers. *Oecologia* **18**:1–16.
- Ryan MG, Yoder BJ (1997) Hydraulic limits to tree height and tree growth. *BioSci* **47**:235–42.
- Sandholt I, Rasmussen K, Andersen J (2002) A simple interpretation of the surface/temperature/vegetation index space for assessment of surface moisture status. *Remote Sens Environ* **79**:213–24.
- Schultz GA (1996) Remote sensing applications to hydrology: runoff/ applications. *Hydrol Sci J* **41**:453–75.
- Schulze E, Kelliher FM, Korner C, *et al.* (1994) Relationships among maximum stomatal conductance, ecosystem surface conductance, carbon assimilation rate, and plant nitrogen nutrition: a global ecology scaling exercise. *Annu Rev Ecol Syst* **25**:629–62.
- Sellers PJ, Berry JA, Collatz GJ, *et al.* (1992) Canopy reflectance, photosynthesis, and transpiration. III. A reanalysis using improved leaf models and a new canopy integration scheme. *Remote Sens Environ* **42**:187–216.
- Slatyer RO, Morrow PA (1977) Altitudinal variation in photosynthetic characteristics of snow gum, *Eucalyptus pauciflora* Sieb. ex Spreng. I. Seasonal changes under field conditions in the Snowy Mountain area of south-eastern Australia. *Austr J Bot* **25**:1–20.
- Smith M-L, Ollinger SV, Martin ME, *et al.* (2002) Direct estimation of aboveground forest productivity through hyperspectral remote sensing of canopy nitrogen. *Ecol Appl* **12**:1286–302.
- Smith WK, Young DR, Carter GA, *et al.* (1984) Autumn stomatal closure in six conifer species of the Central Rocky Mountains. *Oecologia* **63**:237–42.
- Soares JV, Almeida AC (2001) Modeling the water balance and soil water fluxes in a fast growing Eucalyptus plantation in Brazil. *J Hydrol* **253**:130–47.
- Sperry JS (2000) Hydraulic constraints on plant gas exchange. *Agric For Meteorol* **104**:13–23.
- Stape JL, Binkley D, Jacobs WS (2006) A twin-plot approach to determine nutrient limitation and potential productivity in Eucalyptus plantations at landscape scales in Brazil. *For Ecol Manage* **223**:358–62.
- Strain BR, Higginbotham KO, Mulroy JC (1976) Temperature preconditioning and photosynthetic capacity of *Pinus taeda* L. *Photosynthetica* **10**:47–53.
- Sun G, Zhou G, Zhang Z, *et al.* (2006) Potential water yield reduction due to forestation across China. *J Hydrol* **328**:548–58.
- Sun OJ, Sweet GB, Whitehead D, Buchan GD (1995) Physiological responses to water stress and waterlogging in *Nothofagus* species. *Tree Physiol* **15**:629–38.
- Treuhaft RN, Chapman BD, dos Santos JR, *et al.* (2009) Vegetation profiles in tropical forests from multibaseline interferometric synthetic aperture radar, field, and lidar measurements. *J Geophys Res* **114**:D23110.
- Vertessy RA, Watson FGR, Sullivan SK (2001) Factors determining relations between stand age and catchment water balance in mountain ash forests. *For Ecol Manage* **143**:13–26.

- Walcroft AS, Silvester WB, Grace JC, *et al.* (1996) Effects of branch length on carbon isotope discrimination in *Pinus radiata*. *Tree Physiol* **16**:281–6.
- Wang J, White K, Robinson GJ (2000) Estimating surface net solar radiation by use of Landsat-5TM and digital elevation models. *Remote Sens Environ* **21**:31–43.
- Waring RH (2000) A process model analysis of environmental limitations on growth of Sitka spruce plantations in Great Britain. *Forestry* **73**:65–79.
- Waring RH, Cleary BD (1967) Plant moisture stress: evaluation by pressure bomb. *Science* **155**:1248–54.
- Waring RH, Coops NC, Landsberg JJ (2010) Improving predictions of forest growth using the 3-PGS model with observations made by remote sensing. *For Ecol Manage* **259**:1722–9.
- Waring RH, Franklin JF (1979) Evergreen coniferous forests of the Pacific Northwest. *Science* **204**:1380–6.
- Waring RH, Schroeder PE, Oren R (1982) Application of the pipe model theory to predict canopy leaf area. *Can J For Res* **12**:556–60.
- Waring RH, Silvester WB (1994) Variation in $\delta^{13}\text{C}$ values within the tree crowns of *Pinus radiata*. *Tree Physiol* **14**:1203–13.
- Waring RH, Way JB, Hunt R Jr, *et al.* (1995) Remote sensing with synthetic aperture radar in ecosystem studies. *BioScience* **45**:715–23.
- Way DA, Oren R (2010) Differential responses to changes in growth temperature between trees from different functional groups and biomes: a review and synthesis of data. *Tree Physiol* **30**:669–88.
- Whitley R, Medlyn B, Zeppel M, *et al.* (2009) Comparing the Penman–Monteith equation and a modified Jarvis–Stewart model with an artificial neural network to estimate stand-scale transpiration and canopy conductance. *J Hydrol* **373**:256–373.
- Zhao M, Running SW (2010) Drought-induced reduction in global terrestrial net primary production from 2000 through 2009. *Science* **329**:940–3.
- Zhang Q, Middleton EM, Margolis HA, *et al.* (2009) Can a satellite-derived estimate of the fraction of PAR absorbed by chlorophyll (FAPARchl) improve predictions of light-use efficiency and ecosystem photosynthesis for a boreal aspen forest? *Remote Sens Environ* **113**:880–8.
- Zhang Q, Xiao X, Brasell B, *et al.* (2005) Estimating light absorption by chlorophyll, leaf and canopy in a deciduous broadleaf forest using MODIS data and a radiative transfer model. *Remote Sens Environ* **99**:357–71.